Research Article | Vol. 32, No. 26 / 16 Dec 2024 / Optics Express 47296
Optics EXPRESS

Anisotropic below bandgap harmonic generation in β-gallium oxide

MUKHTAR HUSSAIN,[1,2,*] ANDRÉ MESQUITA ANTUNES,[1,3] GONÇALO VAZ,[1] JOANA ALVES,[1,4] HUGO PIRES,[1] TAYYAB IMRAN,[5] MARCO PERES,[6] KATHARINA LORENZ,[6] ENCARNACIÓN VÍLLORA,[7] KIYOSHI SHIMAMURA,[7] SAIBABU MADAS,[8] MOUSUMI UPADHYAY KAHALY,[8] SUBHENDU KAHALY,[8] GONÇALO FIGUEIRA,[1] MARTA FAJARDO,[1] AND GARETH WILLIAMS[1]

[1]*GoLP/Instituto de Plasmas e Fusão Nuclear-Laboratório Associado, Instituto Superior Técnico, Universidade de Lisboa, 1049-001 Lisboa, Portugal*
[2]*Biodesign Center for Applied Structural Discovery, Arizona State University, Tempe, AZ 85287-5001, USA*
[3]*Leiden Institute of Advanced Computer Science, Universiteit Leiden, Einsteinweg 55, 2333CC Leiden, The Netherlands*
[4]*NKT Photonics A/S, Blokken 84, Birkerød 3460, Denmark*
[5]*Extreme Light Infrastructure-Nuclear Physics (ELI-NP), Horia Hulubei National R & D Institute for Physics and Nuclear Engineering (IFIN-HH), 30 Reactorului Street, 077125 Mägurele, jud. Ilfov, Romania*
[6]*Instituto de Engenharia de Sistemas e Computadores - Microsistemas e Nanotecnologia, Rua Alves Redol 9, Lisbon 1000-029, Portugal*
[7]*National Institute for Materials Science, 1-1 Namiki, Tsukuba 305-0044, Japan*
[8]*ELI ALPS, ELI-HU Non-Profit Ltd., Wolfgang Sandner utca 3, Szeged 6728, Hungary*
[*]*mukhtar.hussain@asu.edu*

Abstract: Harmonic generation in wide bandgap semiconductors and dielectrics has attracted a surge of interest as a compact solid-state light source and as a method of mapping the band structure of the material itself. Longer driving wavelengths can support longer electron trajectories and suppress interband transitions, yielding spectra sensitive to crystal orientation and band shapes. Here, we combine a long wavelength laser to drive harmonic generation in a wide band-gap material with applications in photonics and power electronics, beta-gallium oxide (β-Ga_2O_3). We generate harmonics up to the ninth order (H9=3.7 eV) in air, with a ≈ 3.0 μm, 100 kHz, 40 fs mid-infrared (MIR) driving laser in (100) and (010) oriented single crystals of β-Ga_2O_3. We observe odd and even harmonics, spectral interference, and the strong anisotropic response of both odd and even harmonics to the incident laser polarization. Our results are explained in terms of the electronic structure and macroscopic optical properties of β-Ga_2O_3.

© 2024 Optica Publishing Group under the terms of the Optica Open Access Publishing Agreement

1. Introduction

Non-perturbative high harmonic generation (HHG) has been routinely performed in solids [1–7] yielding a new perspective for probing the periodic potential of crystals [8], opening up applications in attosecond science [9] and offering a path to solid-state extreme ultraviolet (XUV) tabletop light sources [2,3,10]. The physical mechanism of HHG in solids is largely attributed to two mechanisms: interband transitions (transition between two real energy levels) and intraband currents (oscillations of the electron within the band) [2]. Studies have shown that the above band-gap harmonics from mid-infrared laser interaction with solids come predominantly from interband transitions [11]. In contrast, the intraband transitions [12] lead to harmonics whose energies are below the bandgap of solids, known as below bandgap harmonics. However, simulation results showed that the below bandgap harmonics originated from both the interband and intraband current [13], making it challenging to disentangle the physical mechanism responsible for any

#525696 https://doi.org/10.1364/OE.525696
Journal © 2024 Received 4 Apr 2024; revised 3 Jun 2024; accepted 13 Jul 2024; published 12 Dec 2024

Optics EXPRESS

given harmonic. β-Ga_2O_3 has attracted considerable interest due to its wide bandgap energy (E_g = 4.8 eV) [14], high thermal stability, high breakdown field, and electron mobility [15]. Therefore, it is an attractive candidate for high-power electronic devices [16] and a promising laser crystal element due to its low phonon energy and good thermal properties [17]. β-Ga_2O_3 is transparent in the ultraviolet to visible wavelength range and attracts attention in the design of optoelectronic devices at shorter wavelengths [18–20]. Thus, the high electron mobility and wide bandgap, along with strong nonlinear optical properties [21], make the β-Ga_2O_3 promising for high-frequency electronic devices, such as field-effect transistors and high-frequency amplifiers. Recently, third-harmonic generation (THG) has been characterized quantitatively to disentangle the surface and bulk contribution in ultra-thin Beta-gallium oxide (β-Ga_2O_3) crystals, highlighting its applications in non-linear optics [22].

Low-order harmonics have many applications ranging from the probing of surface properties [23], non-invasive inspection of interlayer defects [24] to nanoscale light manipulation [25], and detection and characterization of biomolecular changes [26]. These applications drive the search for new robust sources, making β-Ga_2O_3 an intriguing candidate for solid-state harmonic generation.

Here, we report the first study of HHG in β-Ga_2O_3 in the non-perturbative regime. We use (100) and (010) oriented β-Ga_2O_3 crystals to generate below bandgap harmonics using a driving wavelength of $\approx$ 3.0 μm, a 40 fs pulse duration and at a repetition rate of 100 kHz. We observe odd and even harmonic orders, spectral fringes, and a highly anisotropic polarisation response. We explain our measurements in terms of propagation effects and the physics of the generation process.

2. Experimental setup

The schematic of the experimental setup to generate below bandgap harmonics in (100) and (010) oriented single crystals of β-Ga_2O_3 at mid-infrared (MIR) is shown in Fig. 1(a). The spatial and

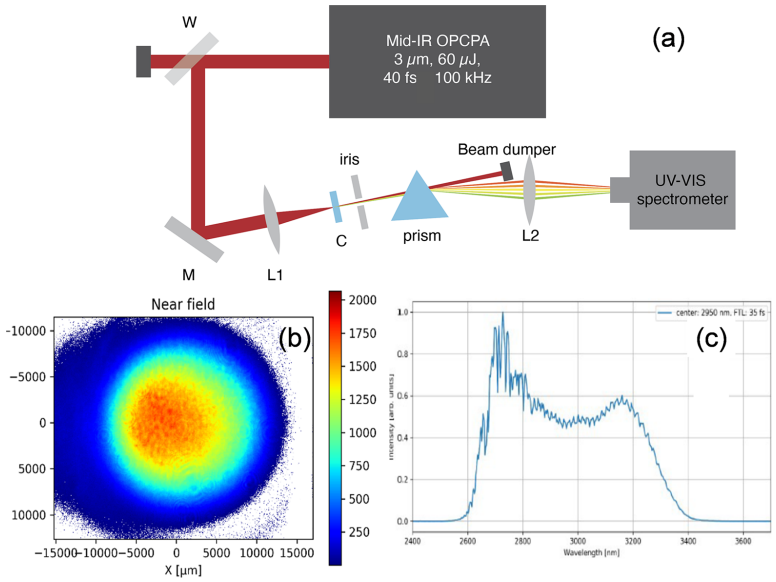

Fig. 1. (a) Schematic illustration of the experimental setup to generate harmonics in (100) and (010) oriented single crystals β-Ga_2O_3 at a driving wavelength of $\approx$ 3.0 μm. (b) Spatial profile of the MIR pulses recorded after the wedge by CCD camera. (c) Spectrum of the MIR laser, spectral ranging from 2.6 μm to 3.3 μm with Fourier transform limited of 35 fs. Here, IR: infrared, W: wedge M: mirror, C: crystal, L1 and L2: lenses.

Optics EXPRESS

spectral profile of the MIR laser are shown in Fig. 1 (b) and Fig. 1 (c), respectively. The spectrum of the MIR laser extends from roughly 2.6 μm to 3.3 μm. The pulse duration is 4-optical cycles. The MIR pulses of $\approx$ 3.0 μm, 40 fs and operating at 100 kHz are focused with a 7.5 cm focal length lens (L1) (Calcium fluoride, CaF_2) to a beam waist radius of $\approx$ 18.0 μm at the surface of the β-Ga_2O_3 crystals. An estimated peak intensity of $\approx 1 \times 10^{13}$ Wcm^{-2} was used to measure harmonics up to ninth-order (H9).

Two commercial, undoped single crystalline β-Ga_2O_3 samples with thicknesses of 650 μm and 500 μm, and with (010) and (100) surface orientations, respectively, were grown using the floating zone technique [27] and supplied by the Tamura company. The dispersion of an ultrafast prism separates the generated harmonics which are then collimated to a UV-VIS spectrometer with a 5.0 cm focal length lens (L2), see Fig. 1(a). The beam dumper blocks the transmitted MIR pulses and the corresponding second harmonic pulses.

3. Results and discussions

3.1. Spectral measurement of harmonics

The spectral measurements of below bandgap harmonics in (100) and (010) oriented single crystals β-Ga_2O_3 at MIR driving wavelength are shown in Figs. 2(a) and 2(b), respectively. Surprisingly, both even and odd harmonics are observed in the spectra. β-Ga_2O_3 belongs to the family of the monoclinic space group $C_{2/m}$ [28], possesses mirror and inversion symmetry [29,30] which supports only the bulk generation of odd-order harmonics. Thus, the observed even-order harmonics are generated from the surface where symmetry is broken [31]. Due to the prism and lens arrangement used to measure the spectrum, the relative intensities of the harmonic spectra are not comparable, but an overall diminishing signal with higher-order harmonics was found.

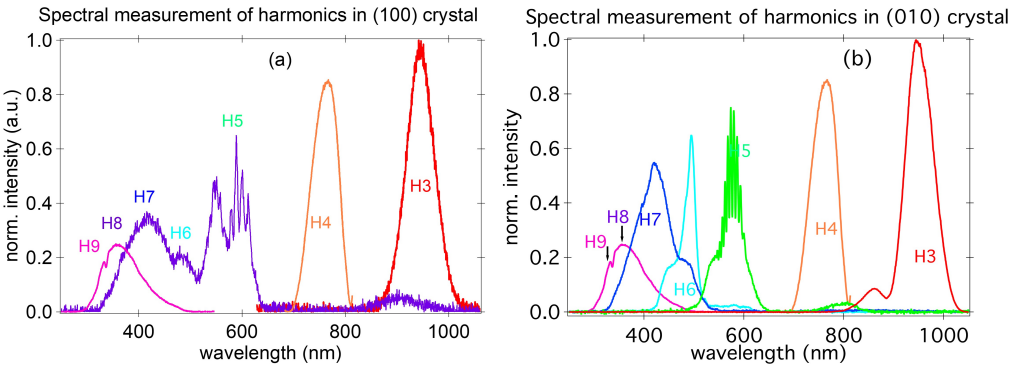

Fig. 2. Spectral measurements of below bandgap harmonics in (100) and (010) oriented single crystals β-Ga_2O_3 at $\approx$ 3.0 μm driving wavelength at an estimated peak intensity of $\approx 1 \times 10^{13}$ W cm^{-2}. (a) (100) β-Ga_2O_3 crystal, acquisition time for H3 is 20 ms, H4 & H5 is 40 ms, H6 & H7 it is 100 ms, while for H8 & H9 it is 200 ms (b) (010) β-Ga_2O_3 crystal, acquisition time for H3, H4, H6 and H7 is 100 ms, while for H5 it is 30 ms and for H8 & H9 is 200 ms.

3.2. Spectral fringes in harmonics

We have observed spectral fringes only in the spectrum of the 3_{rd} (H3), 4_{th} (H4) and 5_{th} (H5) harmonics in both (100) and (010) single crystal β-Ga_2O_3 at $\approx$ 3.0 μm driving wavelength. As H4 can only originate from the surfaces of the crystal due to the symmetry of crystals, we attributed the spectral fringes of H4 to the interference of H4 signal generated from the front and

Optics EXPRESS

back surfaces of the crystals. The spectral fringes of H5 in (100) single crystal are broader with a fringe spacing of ≈ 8 nm, whereas the fringe spacing in the H5 spectrum of (010) single crystal β-Ga_2O_3 crystal is ≈ 6 nm, as shown in Fig. 3(a).

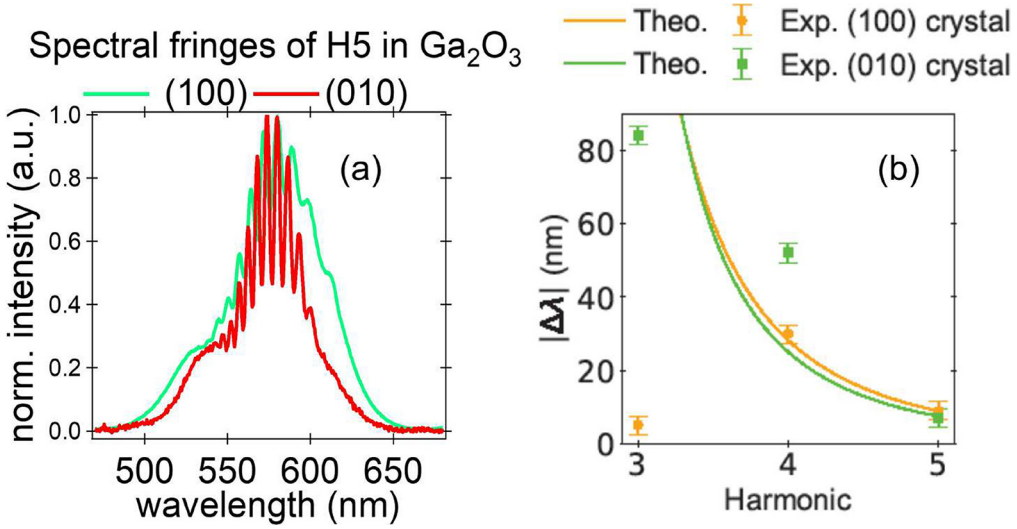

Fig. 3. (a) The spectral fringe measurements of H5 in (100) and (010) oriented single crystals β-Ga_2O_3 at driving wavelengths of ≈ 3.0 μm. (b) Variation of fringe spacing with the order of the harmonics (H3-H5) generated in single crystals of β-Ga_2O_3. The continuous lines correspond to theoretical values calculated from Eq. (1), while the data points correspond to the experimental spacing.

Similar fringes in the spectra of THG and H5 were reported in previous works [32,33], where they were attributed to the interference of two harmonic signals, generated from the front surface and bulk crystal, that propagate with different group velocities leading to a temporal separation at the exit of the bulk. In particular, while one of the signals travels freely the other propagates phase-locked with the pump, thus sharing the same group velocity. As such, the expected fringe spacing for m^{th} harmonic can be calculated as [34]

$$\Delta\lambda = \frac{\lambda^2}{c\Delta t} = \frac{\lambda^2}{c.d.\left(\frac{1}{v_{g,\omega}} - \frac{1}{v_{g,m\omega}}\right)} \tag{1}$$

where c is the speed of light, Δt is the temporal separation between the two harmonic pulses generated at the surface after propagating through the crystal, d is its thickness, $v_{g,\omega}$ and $v_{g,m\omega}$ are the group velocities of the fundamental and m-th-order harmonic pulses, respectively. The group velocity is calculated as $v_g = c/(n - \lambda\frac{dn}{d\lambda})$, where the refractive index (n) is described by Sellmeier equations fitted to data in the 0.407-1.551 μm region [35]. For the case of the observable fringes of H5, we obtain $|\Delta\lambda| \approx 9$ and 7.5 nm for (100) and (010), respectively, which is within expectation for the 8 and 6 nm that we obtained from the experiment. Regarding the lack of fringes for higher harmonics (H7-H9), as $|\Delta\lambda| \approx$ 0.4-1.7 nm, our spectrometer was unable to resolve the peaks since $|\Delta\lambda|$ is below its resolving power.

Figure 3(b) depicts expected and measured values for the fringe spacing in both single crystal samples from H3 to H5. The measured values are close to those predicted except for H3, where the measured values are far inferior to the expected value ($|\Delta\lambda| \approx$ 172-204 nm for (100) and (010), respectively). These distances surpass the bandwidth of the third harmonic and would be

Optics EXPRESS

impossible to observe. However, we do observe higher frequency fringes, corresponding to a longer-than-predicted temporal separation possible due to the birefringence of the samples, as the spacing was sensitive to the sample orientation. The fringe spacing in the spectra is consistent with calculations of the group velocity mismatch of the driving and harmonic pulses, albeit with a large deviation from predictions for H3, due to fringe spacing being wider than the harmonic bandwidth and the presence of secondary frequency modulations from the birefringence of the crystal. By varying material thicknesses and incident laser polarization, the spectral fringes can be observed in solid materials. This spectral interference of fringes could be used to measure the refractive index of different materials over a wide frequency range.

3.3. Orientation dependence of below bandgap harmonics

It has been shown elsewhere that the dependence of harmonic yield is intricately related to the direction of laser polarization relative to the crystal orientation, being particularly sensitive to band structure and atomic positions [3,36,37]. Here, We rotate the β-Ga_2O_3 crystal about its axis while keeping the laser's linear polarization unchanged to the crystals' surface plane. Insets of Fig. 4 show the crystal structure of Ga_2O_3 with the stick and ball model illustrating the unit cell of Ga_2O_3 along with the atomic positions in (010) and (100) surface plane orientation. The gallium (Ga) and oxygen (O) atoms are represented by red and blue balls, respectively.

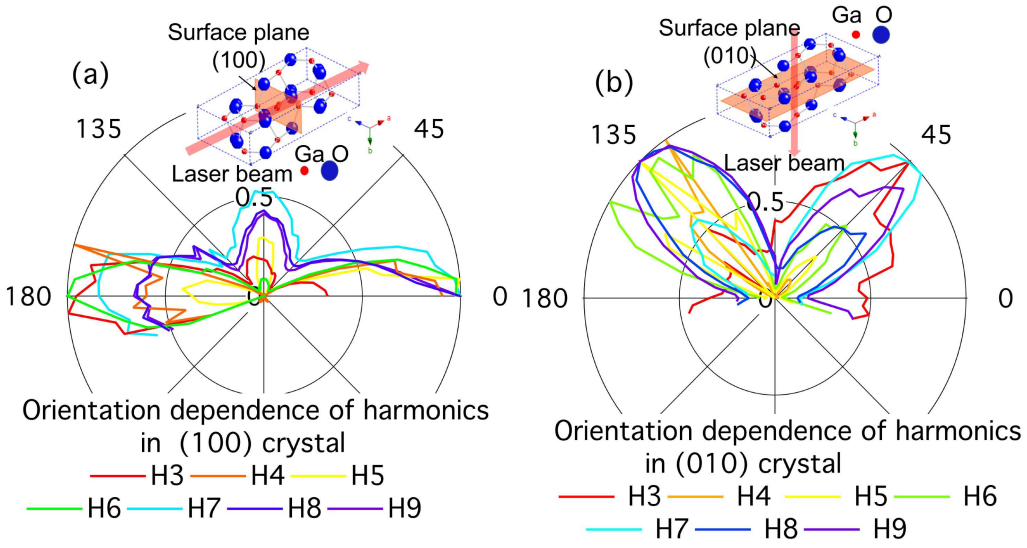

Fig. 4. Orientation dependence of below bandgap harmonics at $\approx 3.0\ \mu$m driving wavelength in single crystals β-Ga_2O_3 with different orientations, (a) (100) oriented crystal, (b) (010) oriented crystal. Insets showed the crystal structure of Ga_2O_3: Stick and ball model illustrating the unit cell of Ga_2O_3 along with the atomic positions in (010) and (100) plane. The gallium (Ga) and oxygen (O) atoms are represented by red and blue balls, respectively, with the laser beam propagation through the surface plane of the crystals.

A two-fold anisotropic polarization of harmonics H3 and H4 has been observed in both (100) and (010) β-Ga_2O_3 at lower intensities, and attributed to Kerr-type harmonics and a photoluminescence signal, respectively. The two-fold polarization response of H3 is linked to the twofold crystal structure of β-Ga_2O_3 [22]. Interestingly, a four-fold anisotropic polarization response of higher harmonics (H5 to H9) has been observed in (100) and (010) β-Ga_2O_3 crystal.

Optics EXPRESS

The even and odd-order harmonics observed from the β-Ga_2O_3 crystals are qualitatively similar, indicating a similar generation mechanism within the surface and bulk. Despite the overall similarity, some notable differences exist between the responses for different harmonics discernible from noise. Namely, in Fig. 4(a) the signal along the 0° to 180° direction for the (100) crystal appears for all harmonics, whereas along the 90° to 270° direction the signal has a strong dependence on harmonic order and is absent for H4 and generally increases for higher orders. For the (010) crystal in Fig. 4(b) the pattern is in general shifted 45° relative to the (100) crystal as shown in Fig. 4(a), and only a very small signal apparent for H4 along the 45° to 225° direction. The dependence tends towards a nearly four-fold symmetrical pattern for H7-H9. Studies on multiphoton absorption in β-Ga_2O_3 have shown a distinct two-lobe intensity structure in the polar plots [38]. Other works have shown similar patterns for second harmonic generation in β-Ga_2O_3, and attributed it to symmetry breaking from the surface or local defects [39]. Furthermore, the polar response in HHG in solids has been shown to follow closely the multiphoton absorption probability as a function of angle [40]. Owing to similar responses for both the even and odd harmonics and the similar multiphoton absorption patterns for β-Ga_2O_3 and their link to the HHG polar response, we attribute this pattern to an angular sensitivity to multiphoton absorption which then gives rise to perturbative harmonics from the surfaces (even harmonics) and bulk (odd harmonics). Considering the low photon energy of the driving laser and the below band gap photon energies, the dominant HHG mechanism is most likely to be intraband oscillations.

3.4. TDDFT calculations of below bandgap harmonics in β-Ga_2O_3

We modeled below bandgap harmonic generation in bulk β-Ga_2O_3 with an *ab initio* TDDFT, using the open-source Octopus package [41–43] to support the experimental findings. The approach is completely from first principles, requiring only a few intuitive approximations to make the calculations tractable, having also shown promising results for modelling solid-state HHG [44–46].

We solve the time-dependent Kohn-Sham (KS) in a real-space grid, with an added driving laser pulse described by its vector potential $\mathbf{A}(t)$, in the velocity gauge, within the dipole approximation (in atomic units):

$$-i\frac{\partial \varphi_i}{\partial t}(\mathbf{r},t) = \left(\frac{1}{2}\left(-i\nabla + \frac{\mathbf{A}(t)}{c}\right)^2 + V_{\mathrm{KS}}[n](\mathbf{r},t)\right)\varphi_i(\mathbf{r},t), \tag{2}$$

where the φ_i are the time-dependent KS orbitals, and $V_{\mathrm{KS}}[n]$ is the effective KS potential, a functional of the electron density $n(\mathbf{r},t)$. The potential includes an external Coulomb (ionic) term, the mean-field Hartree electrostatic potential, and the exchange-correlation term. After the calculation, the harmonic spectrum can be recovered from the time-dependent electronic current density $\mathbf{j}(\mathbf{r},t)$, integrated over the volume of the crystal's modelled unit cell Ω:

$$\mathrm{HHG}(\omega) = \left|\mathrm{FT}\left(\int_\Omega \frac{\partial}{\partial t}\mathbf{j}(\mathbf{r},t)d^3r\right)\right|^2, \tag{3}$$

where FT denotes the Fourier Transform.

The adiabatic local density approximation (LDA) was employed, and norm-conserving Hartwigsen-Gödecker-Hutter pseudopotentials were used for the calculation.

We used a 4×16×8 **k**-grid for the higher intensity, and a 3×13×7 **k**-grid for the lower intensity. This was chosen based on its efficacy in suitably representing the Brillouin Zone (BZ) of β-Ga_2O_3, while capturing the essential electron dynamics induced by the laser field intensity at a reduced computational cost. We used a real-space grid spacing and a time step of 0.3 and 0.2 atomic units, respectively.

Optics EXPRESS

The laser pulse parameters were set to match those of the experiment: a 3.0 μm central wavelength, FWHM duration of 40 fs, and we opted for a $\sin^2$ temporal envelope for numerical convenience. The peak intensity in the simulations must be compensated to account for 1) the reflective losses at the surface; 2) the peak electric field decrease due to the material's refractive index; and 3) the underestimation of the bandgap energy that is characteristic of the LDA exchange-correlation functional. This final step equates to conserving the experimental effective Keldysh parameter [47].

Using estimated and averaged (due to the material's birefringence) values of the refractive index and the Fresnel reflection coefficient [48], and considering the DFT and measured bandgap energies of 2.28 eV and 4.85 eV [49], respectively, the resulting peak intensity starting from the experimental $\approx 1.0 \times 10^{13}$ W cm^{-2} drops to around $\approx 1.7 \times 10^{12}$ W cm^{-2}. This scaling is an approximate compensation between experimental intensity and that used in TD-DFT, therefore we present a spectrum with the corrected intensity and also with a higher driving intensity of $\approx 5.2 \times 10^{12}$ W cm^{-2} in Fig. 5. The resulting harmonic spectra are shown in Fig. 5. A significant amount of spectral noise observed, especially in the short wavelength part of the spectrum, is common in TDDFT simulations of solid-state HHG, arising from the exclusion of decoherence effects from scattering events in the standard implementation of Octopus [50,51]. This effect makes the harmonic peaks of orders higher than the fifth difficult to identify. However, the third and fifth harmonic peaks are between one to two orders of magnitude greater than the intensity in the region where the fourth harmonic would be present, consistent with odd harmonic generation supported in a centrosymmetric crystal such as β-Ga_2O_3.

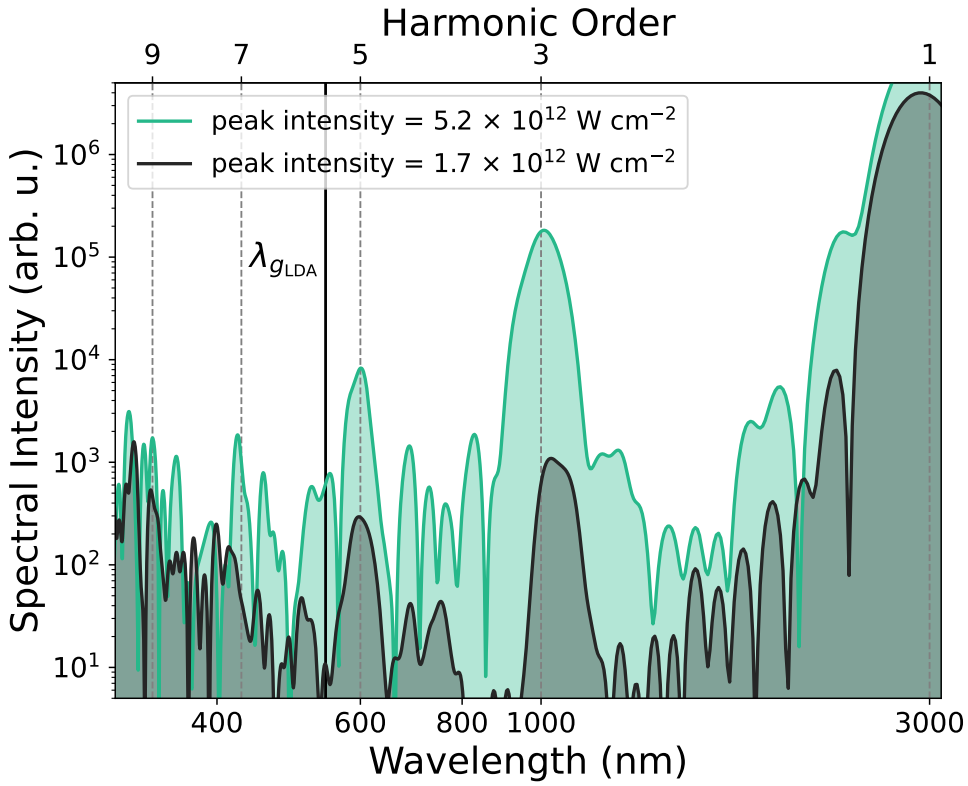

Fig. 5. Bulk β-Ga_2O_3 harmonic spectra from TDDFT simulations. The driving laser polarization was aligned with the crystallographic b-axis, establishing an equivalence with experimental normal incidences to the (100)-cut single crystal. $\lambda_{g_{\mathrm{LDA}}}$ is the wavelength corresponding to the DFT-calculated bandgap energy.

Optics EXPRESS

In Fig. 6 we present the normalised harmonic intensity for various angles of linear polarisation of the driving field relative to the crystal for the intensity of $\approx 5.2 \times 10^{12}$ W cm^{-2}. For H3 a relatively homogeneous response is observed compared to the higher harmonics. The higher orders (H5, H7 and H9) present sharp lobes at 0° and 180°, with various levels of emission at 90° and 270°. These higher harmonics follow the general trend seen in the experiment (Fig. 4). The exception is H3 which presents a broader response which is typical of Kerr-like harmonics. This difference can be due to many factors in the model, such as the ground state bandstructure, incorrect bandgap, or incorrect intensity scaling. However, the agreement with the higher orders is encouraging and shows the model capturing the general behaviour observed in the experiment.

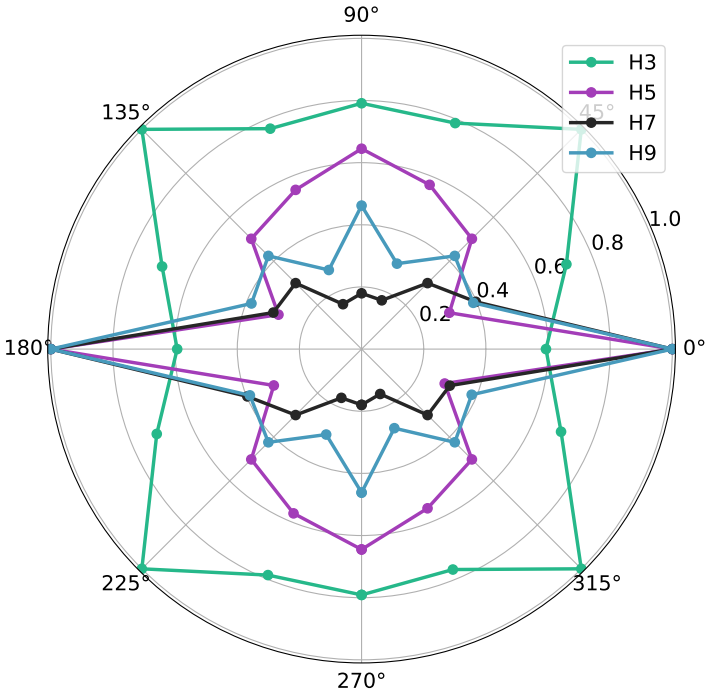

Fig. 6. Orientation dependence of the (normalized) harmonic yield in bulk β-Ga_2O_3 from TDDFT simulations, with a driving field peak intensity of 5.2×10^{12} W cm^{-2}. The yields mapped onto the 0° and 90° directions correspond to driving laser polarizations aligned with the c and b crystal axes, respectively, with all remaining angles lying in the (100) crystallographic plane (cf. Figure 4 (a)).

4. Conclusion

We have generated even and odd harmonics up to H9 using a laser with ≈ 3.0 μm driving wavelength in β-Ga_2O_3 crystals. Spectral fringes were observed and attributed to the spectral interference of two temporally shifted pulses generated from the front surface and within the bulk of the crystals for both even and odd harmonics. Analysis of the measured fringe spacing and those predicted from available data on the refractive index support this claim. Upon rotation of the crystal relative to the laser linear polarization, an anisotropic orientation dependence of harmonic intensity was observed in (100) and (010) oriented β-Ga_2O_3 crystals for all harmonics. The anisotropic harmonics pattern rotates 45° when changing from the (100) to (010) crystal, highlighting the sensitivity of the high harmonics process on the crystallographic properties and band structure. We attribute the angular response to the changing probability of multiphoton

Optics EXPRESS

absorption of the driving laser as the sample is rotated. This is supported both by the available literature and our data, which shows an overall similar angular response for odd and even harmonics which can only come from a process common to both mechanisms, multiphoton absorption. This work has shown that β-Ga_2O_3 is a robust crystal for below bandgap odd and even harmonic generation at a $\approx$3.0 μm up to the 9^{th} harmonic in air and could be a potential candidate for ultraviolet sources and optical probing of the crystal or band structures.

Funding. Ministerstvo Školství, Mládeže a Tělovýchovy (90254); Fundação para a Ciência e a Tecnologia (2022.00804 CEECIND, 2022.05329.PTDC, 2022.09213.PTDC); European Commission (GINOP-2.3.6-15-2015-00001); Fundação para a Ciência e a Tecnologia (LA/P/0061/202, PD/BD/135177/2017, PD/BD/135224/2017, UIDB/50010/2020).

Disclosures. The authors declare no conflicts of interest.

Data availability. Data underlying the results presented in this paper are available in Ref. [52].

References

1. S. Ghimire, A. D. DiChiara, E. Sistrunk, *et al.*, "Observation of high-order harmonic generation in a bulk crystal," Nat. Phys. **7**(2), 138–141 (2011).
2. S. Ghimire and D. A. Reis, "High-harmonic generation from solids," Nat. Phys. **15**(1), 10–16 (2018).
3. Y. S. You, D. A. Reis, and S. Ghimire, "Anisotropic high-harmonic generation in bulk crystals," Nat. Phys. **13**(4), 345–349 (2017).
4. Y. S. You, Y. Yin, Y. Wu, *et al.*, "High-harmonic generation in amorphous solids," Nat. Commun. **8**(1), 724 (2017).
5. G. Vampa, B. Ghamsari, S. S. Mousavi, *et al.*, "Plasmon-enhanced high-harmonic generation from silicon," Nat. Phys. **13**(7), 659–662 (2017).
6. M. Wu, Y. You, S. Ghimire, *et al.*, "Orientation dependence of temporal and spectral properties of high-order harmonics in solids," Phys. Rev. A **96**(6), 063412 (2017).
7. H. Liu, Y. Li, Y. S. You, *et al.*, "High-harmonic generation from an atomically thin semiconductor," Nat. Phys. **13**(3), 262–265 (2017).
8. Y. S. You, E. Cunningham, D. A. Reis, *et al.*, "Probing periodic potential of crystals via strong-field re-scattering," J. Phys. B: At., Mol. Opt. Phys. **51**(11), 114002 (2018).
9. J. Li, J. Lu, A. Chew, *et al.*, "Attosecond science based on high harmonic generation from gases and solids," Nat. Commun. **11**(1), 1–13 (2020).
10. V. E. Nefedova, S. Fröhlich, F. Navarrete, *et al.*, "Enhanced extreme ultraviolet high-harmonic generation from chromium-doped magnesium oxide," Appl. Phys. Lett. **118**(20), 201103 (2021).
11. S. Y. Kruchinin, F. Krausz, and V. S. Yakovlev, "Colloquium: Strong-field phenomena in periodic systems," Rev. Mod. Phys. **90**(2), 021002 (2018).
12. F. Schlaepfer, M. Lucchini, S. A. Sato, *et al.*, "Attosecond optical-field-enhanced carrier injection into the gaas conduction band," Nat. Phys. **14**(6), 560–564 (2018).
13. Y.-T. Zhao, S.-C. Jiang, X. Zhao, *et al.*, "Effect of interband polarization on a solid's high-order-harmonic generation just belowthe band gap," Opt. Lett. **45**(10), 2874–2877 (2020).
14. H. Tippins, "Optical absorption and photoconductivity in the band edge of β- ga 2 o 3," Phys. Rev. **140**(1A), A316–A319 (1965).
15. S. Poncé and F. Giustino, "Structural, electronic, elastic, power, and transport properties of β- ga 2 o 3 from first principles," Phys. Rev. Res. **2**(3), 033102 (2020).
16. J. Zhang, J. Shi, D.-C. Qi, *et al.*, "Recent progress on the electronic structure, defect, and doping properties of ga2o3," APL Mater. **8**(2), 020906 (2020).
17. W. Mu, Y. Yin, Z. Jia, *et al.*, "An extended application of β-ga 2 o 3 single crystals to the laser field: Cr 4+: β-ga 2 o 3 utilized as a new promising saturable absorber," RSC Adv. **7**(35), 21815–21819 (2017).
18. N. Ueda, H. Hosono, R. Waseda, *et al.*, "Synthesis and control of conductivity of ultraviolet transmitting β-ga 2 o 3 single crystals," Appl. Phys. Lett. **70**(26), 3561–3563 (1997).
19. M. Orita, H. Ohta, M. Hirano, *et al.*, "Deep-ultraviolet transparent conductive β-ga 2 o 3 thin films," Appl. Phys. Lett. **77**(25), 4166–4168 (2000).
20. J. Zhou, H. Chen, K. Fu, *et al.*, "Gallium oxide-based optical nonlinear effects and photonics devices," J. Mater. Res. **36**(23), 4832–4845 (2021).
21. H. Chen, H. Fu, X. Huang, *et al.*, "Characterizations of the nonlinear optical properties for (010) and (2 0 1) beta-phase gallium oxide," Opt. Express **26**(4), 3938–3946 (2018).
22. G. Yi, S. Jeon, Y. W. Kwon, *et al.*, "Enhanced third harmonic generation in ultrathin free-standing β-ga 2 o 3 nanomembranes: study on surface and bulk contribution," Nanoscale **14**(1), 175–186 (2022).
23. Y. Shen, "Surface properties probed by second-harmonic and sum-frequency generation," Nature **337**(6207), 519–525 (1989).
24. Y. Gao, H. Lee, J. Jiao, *et al.*, "Surface third and fifth harmonic generation at crystalline si for non-invasive inspection of si wafer's inter-layer defects," Opt. Express **26**(25), 32812–32823 (2018).

Optics EXPRESS

25. W.-Y. Tsai, T. L. Chung, H.-H. Hsiao, *et al.*, "Second harmonic light manipulation with vertical split ring resonators," Adv. Mater. **31**(7), 1806479 (2019).
26. Y. Birman, S. Khorsand, E. Tu, *et al.*, "Second-harmonic generation-based methods to detect and characterize ligand-induced rna conformational changes," Methods **167**, 92–104 (2019).
27. E. G. Víllora, K. Shimamura, Y. Yoshikawa, *et al.*, "Large-size β-ga2o3 single crystals and wafers," J. Cryst. Growth **270**(3-4), 420–426 (2004).
28. S. Geller, "Crystal structure of β-ga2o3," J. Phys. Chem. C **33**(3), 676–684 (1960).
29. L. Li, "Piezoelectric properties of substitutionally doped β-ga2o3," AIP Adv. **11**(6), 1 (2021).
30. M. A. Bryushinin, I. A. Sokolov, R. V. Pisarev, *et al.*, "Space-and-time current spectroscopy of a β-ga 2 o 3 crystal," Opt. Express **23**(25), 32736–32746 (2015).
31. M. Hussain, G. Williams, T. Imran, *et al.*, "Non-linear propagation effects of intense femtosecond pulses on below bandgap harmonics in solids," J. Mod. Opt. **70**(3), 197–204 (2023).
32. M. Hussain, S. Kaassamani, T. Auguste, *et al.*, "Spectral control of high order harmonics through non-linear propagation effects," Appl. Phys. Lett. **119**(7), 071101 (2021).
33. N. Garejev, I. Gražulevičiūtė, D. Majus, *et al.*, "Third-and fifth-harmonic generation in transparent solids with few-optical-cycle midinfrared pulses," Phys. Rev. A **89**(3), 033846 (2014).
34. D. Franz, "High harmonic generation in crystals assisted by local field enhancement in nanostructures," Ph.D. thesis, Paris Saclay (2018).
35. I. Bhaumik, R. Bhatt, S. Ganesamoorthy, *et al.*, "Temperature-dependent index of refraction of monoclinic Ga2O3 single crystal," Appl. Opt. **50**(36), 6606 (2011).
36. M. Hussain, F. Lima, W. Boutu, *et al.*, "Demonstration of nonperturbative and perturbative third-harmonic generation in mgo by altering the electronic structure," Phys. Rev. A **105**(5), 053103 (2022).
37. Z. Long, H. Yang, K. Tian, *et al.*, "High-harmonic generation in cdte with ultra-low pump intensity and high photon flux," Commun. Phys. **6**(1), 228 (2023).
38. J. B. Cho, G. Jung, K. Kim, *et al.*, "Highly asymmetric optical properties of beta-ga2o3 as probed by linear and nonlinear optical excitation spectroscopy," J. Phys. Chem. C **125**(2), 1432–1440 (2021).
39. G. Gutierrez, E. M. Sundin, P. G. Nalam, *et al.*, "Interfacial phase modulation-induced structural distortion, band gap reduction, and nonlinear optical activity in tin-incorporated ga2o3," J. Phys. Chem. C **125**(37), 20468–20481 (2021).
40. P. Juergens, S. D. C. Roscam Abbing, M. Mero, *et al.*, "Linking high-harmonic generation and strong-field ionization in bulk crystals," ACS Photonics **11**(1), 247–256 (2024).
41. M. Marques, "octopus: a first-principles tool for excited electron-ion dynamics," Comput. Phys. Commun. **151**(1), 60–78 (2003).
42. A. Castro, H. Appel, M. Oliveira, *et al.*, "octopus: a tool for the application of time-dependent density functional theory," Phys. Status Solidi B **243**(11), 2465–2488 (2006).
43. N. Tancogne-Dejean, M. J. T. Oliveira, X. Andrade, *et al.*, "Octopus, a computational framework for exploring light-driven phenomena and quantum dynamics in extended and finite systems," J. Phys. Chem. C **152**(12), 124119 (2020).
44. N. Tancogne-Dejean, O. D. Mücke, F. X. Kärtner, *et al.*, "Impact of the electronic band structure in high-harmonic generation spectra of solids," Phys. Rev. Lett. **118**(8), 087403 (2017).
45. N. Tancogne-Dejean, O. D. Mücke, F. X. Kärtner, *et al.*, "Ellipticity dependence of high-harmonic generation in solids originating from coupled intraband and interband dynamics," Nat. Commun. **8**(1), 1–10 (2017).
46. Z. Nourbakhsh, N. Tancogne-Dejean, H. Merdji, *et al.*, "High harmonics and isolated attosecond pulses from mgo," Phys. Rev. Appl. **15**(1), 014013 (2021).
47. V. E. Gruzdev, *Laser-induced ionization of solids: back to keldysh* (SPIE, 2005), p. 480–492.
48. S. Stepanov, V. Nikolaev, V. Bougrov, *et al.*, "Gallium oxide: Properties and applica 498 a review," Rev. Adv. Mater. Sci **44**, 63–86 (2016).
49. S. J. Pearton, J. Yang, P. H. Cary, *et al.*, "A review of ga_2o_3 materials, processing, and devices," Appl. Phys. Rev. **5**(1), 011301 (2018).
50. I. Floss, C. Lemell, G. Wachter, *et al.*, "Ab initio multiscale simulation of high-order harmonic generation in solids," Phys. Rev. A **97**(1), 011401 (2018).
51. I. Floss, C. Lemell, K. Yabana, *et al.*, "Incorporating decoherence into solid-state time-dependent density functional theory," Phys. Rev. B **99**(22), 224301 (2019).
52. M. Hussain, A. M. Antunes, G. Vaz, *et al.*, "Anisotropic below bandgap harmonic generation in β-gallium oxide," Optica Open (2024).

144.213.253.16 {ts '2024-12-12 20:02:06'}